

ABSTRACT

Weak non-covalent interactions play important role in many chemical and biological processes. As a matter of fact, the phenomenon of “Molecular Recognition” is dominated by weak forces, which include H-bonding, electrostatic, stereo-electronic, π -stacking and related hydrophobic interactions. In the biological world, maintenance of protein’s secondary structure is governed by such weak forces. The, nucleic acids are no exceptions. Weak forces also play a major role in the biological activity of various naturally occurring compounds, as for example, in naturally occurring enediynes, these forces play a crucial role in controlling their reactivity towards Bergman Cyclization. Such weak interactions also play a vital role in determining the reactivity and recognition processes in β -lactam antibiotics. Besides these electronic and other interactions, the strain imposed in small 4-membered heterocyclic ring β -lactam also plays a dominant role.

This dissertation has focused on the role of such weak forces in controlling the conformation and reactivity of two particularly important pharmacophores, namely the enediynes and β -lactams. The possible use of enediyne framework as a scaffold for peptidomimetics was also explored.

1. THE ROLE OF ELECTROSTATIC AND H-BONDING INTERACTIONS ON THE KINETICS OF BERGMAN CYCLIZATION IN ENEDIYNYL AMINO ACIDS AND PEPTIDES

A careful survey of the various reports in the literature revealed that a major thrust in the enediyne research has been the design and synthesis of novel mimics of the natural enediynes and evaluation of their biological and chemical activities. Through extensive research inputs over the past years, it became clear that cyclic enediynes are more reactive than their acyclic counterparts. Thus, apart from directly starting with a cyclic framework; activation of enediynes towards Bergman cyclization (BC) can be achieved by the formation of an *in situ* cyclic moiety.

Thus, we have synthesized the enediynyl ω -amino acids and peptides (1-6) as represented in **Figure 1**. The rationale behind the design of enediynyl ω -amino acids is the likely formation of pseudo cyclic framework *via* intramolecular H-bond or electrostatic interactions between the terminal zwitter ions thereby lowering the c, d-distance and hence the activation barrier for cycloaromatization. Metal ion coordination, in general, has been shown to lower the activation barrier for BC in

acyclic enediynes through metal-ligand interactions. With this in mind, we synthesized the amido enediynes **1-6** and studied their rates of BC.

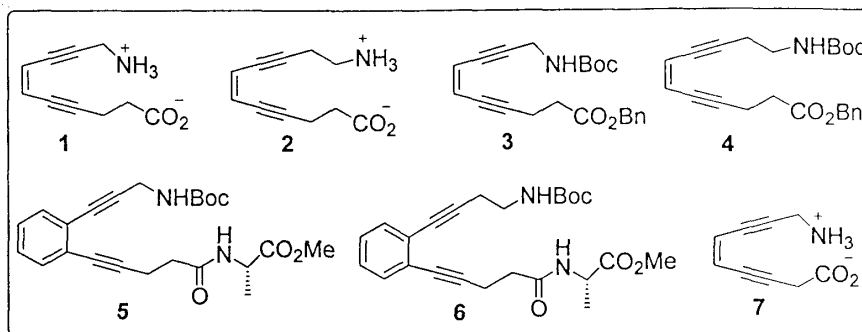


Figure 1: Our target amino acids and peptides

Based on MM2 calculations it is found only in a series like free amino acids (**1, 2** and **7**), protected amino acids (**3** and **4**) and peptides (**5** and **6**), there is a correlation between the reactivity, c-d distances and the various weak interactions like H-bonding, electrostatic etc. Although electrostatic or H-bond interactions will be different in solution phase, still these initial calculations predicted some degree of reactivity differences in these compounds.

Unfortunately, we could not synthesize the amino acid **7** as the Sonogashira coupling involving propargylic esters created problems. The higher homologous acid, 3-butynoic acid could not be used also because of the problem of easy tautomerization to the allenic acid. This prompted us to synthesize the amino acids and the peptides from the commercially available 4-pentynoic acid.

The onset temperatures for BC for these enediynyl amino acids and the peptides were determined using the Differential Scanning Calorimetric (DSC) measurements that were recorded in neat state without any solvent and shown in the **Table 1**.

Solution phase kinetics in DMSO in presence of 1,4-CHD at 150 °C was also carried out, the rate of disappearance of the enediynyl peptides were monitored by HPLC using an internal standard (naphthalene). This also revealed higher reactivity of peptide **5** ($k_{\text{obs}} = 12 \times 10^{-2}$ per h) as compared to peptide **6** ($k_{\text{obs}} = 2.08 \times 10^{-2}$ per h).

Table 1: The onset temperatures of enediynyl amino acids and peptides

Entry	Onset Temp. (DSC)
1	92 °C
2	99 °C
3	111 °C
4	133 °C
5	121 °C
6	207 °C

The large difference of reactivity towards BC have been ascribed to the presence of stronger intramolecular H-bonding involving the carbamate NH and the amide carbonyl in peptide **5** than that for peptide **6** as supported by the variable temperature NMR experiments. The carbamate NH showed very low temperature dependence in d_6 -DMSO and is within the Kessler limit of -3 ppb/K thus proving high degree of intramolecular H-bonding in peptide **5**.

In conclusion, we have been able to demonstrate the importance of H-bonding/electrostatic interactions in lowering the activation energy of BC.

2. SYNTHESIS OF PYRIDAZINEDIONE-BASED ENEDIYNES: ROLE OF HYBRIDIZATION OF REMOTE ATOMS ON THE KINETICS OF BERGMAN CYCLIZATION

Amongst the various strategies, the incorporation of trigonal carbon atoms in bicyclic enediynes in modulating the kinetics of BC has been reported. In fact, the rigid double bond in the bicyclic network of calicheamicin and esperamicin acts as a locking device to stabilize the reactive enediyne system. Pyridazinediones and related compounds do have properties similar to the analogous pyrimidines and pyridazoles. Recently, tetrahydropyridazine scaffold based irbesartan analogs have been shown to have higher binding affinity towards AT₁-receptor.

We planned to synthesize the biologically active pyridazinedione based benzene-fused enediynes **8-9** (Figure 2) to study the chemical reactivity towards Bergman cyclization. We were particularly interested to know whether the reactivity of these enediynes is dependent upon the state of hybridization of C-4 and C-5 atoms of the parent heterocyclic pyridazinedione ring.

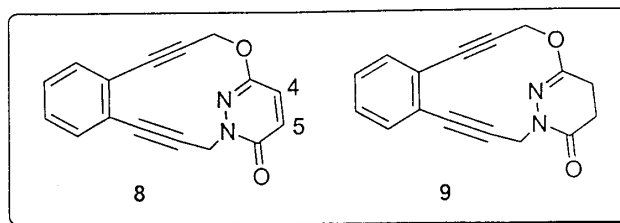


Figure 2: Our target pyridazinedione based enediynes

After establishing the structure of the enediynes **8** and **9**, their reactivity towards Bergman Cyclization (BC) was next studied in both solid and solution phase. The solid phase reactivity was determined by Differential Scanning Calorimetry (DSC), which showed strong exothermic peaks for both the enediynes. The onset temperature for BC for enediyne **8** was ~ 228 °C whereas that for the other enediyne **9**, the onset temperature was at ~ 196 °C after an initial endothermic dip due to melting (Figure 3). Thus the enediyne lacking unsaturation at C-4 and C-5 (of the parent heterocyclic ring) has lower activation barrier when heated in neat state.

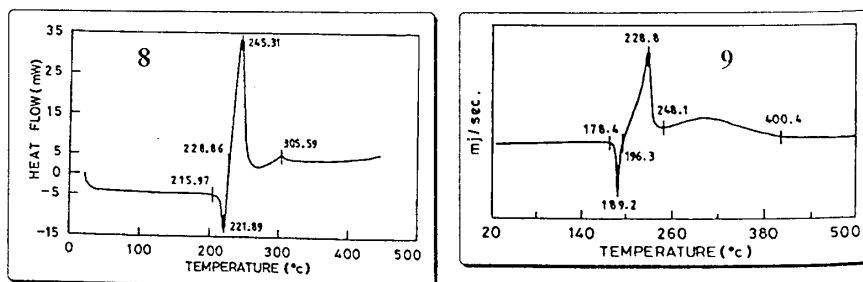


Figure 3: DSC curves of enediyne **8** and **9**

The solution phase kinetics was determined by heating a solution of the enediyne in a sealed tube at a preset temperature in CHCl_3 containing an excess of 1, 4-cyclohexadiene and then taking the $^1\text{H-NMR}$ at different time points. For the tetrahydropyridazinedione enediyne **9**, the half-life, determined at 130 °C, was found to be 120 h. The dihydropyridazinedione enediyne **8** failed to cyclize at all at 130 °C even after heating for 156 h. Finally the half-life was determined at 150 °C and was found to be ~ 200 h. The 1^{st} order rate constants are for **9** at 130 °C and for **8** at 150 °C are 3.55×10^{-2} /h and 3.14×10^{-3} /h respectively. Thus it is demonstrated without any

doubt that enediyne **9** is much more reactive than the corresponding unsaturated compound **8** both in solid state and in solution phase indicating the importance of the state of hybridization of the carbon atoms in the pyridazinedione framework.

The observed difference in reactivity of the two enediynes is obviously not due to the distance factor as the c, d-distances turned out to be almost same (3.79 Å) by X-ray analysis. In order to find out a plausible explanation, we carried out semiempirical¹³ PM5 calculation in the gas phase on both the enediynes.

The activation energy for the formation of product biradical from enediyne **9** came out to be smaller (~8.9 Kcal mol⁻¹) than that of the corresponding product from enediyne **8**. The singlet biradical generated from enediyne **8** is predicted to lie 5.2 Kcal/mol below the corresponding triplet, suggesting that it may be less reactive as a hydrogen-atom-abstracting agent than biradical generated from enediyne **9**, which has a S-T splitting of 3.5 kcal/mol.

Thus we have successfully synthesized pyridazinedione-based enediynes and their structures well characterized. We have also demonstrated the perturbation caused by a remote double bond in the diazine system. Since double bond can be functionalised in several ways so that the carbons become sp³ hybridized, we can expect generation of large library of functionalised enediynes possibility with greater reactivity than the corresponding unsaturated analogue. Similar effects in other heterocyclic systems, especially in pyrimidine and dihydropyrimidine-fused systems may exist.

3. EFFECT OF π -STACKING AND CHARGE TRANSFER INTERACTIONS ON THE KINETICS OF BERGMAN CYCLIZATION

To elaborate the concept of weak interactions and their effect on Bergman Cyclization (BC), we have synthesized some enediyne compounds incorporating Donor and Acceptor units in the two arms of enediynes and followed their charge transfer/ π -stacking interactions. UV/vis spectroscopy was utilized to measure the CT spectroscopic properties.

Specifically, our intention was to investigate the possibility of encouraging Bergman Cyclization (BC) by pulling the reactive centers together with, if possible, CT / π -stacking interactions between the two arms of the enediynes.

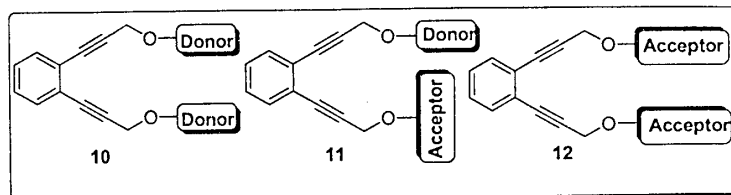


Figure 4: Representation of Donor-Acceptor Containing Enediyns

With this intention, we planned to synthesize and study the spectroscopic properties of a series of enediyne molecules (**Figure 4**), incorporating Donor and Acceptor units in the two arms of the enediynyl moiety. The corresponding D/D and A/A counterparts were also synthesized to compare the reactivities towards Bergman Cyclization. UV/vis spectroscopy was utilized to measure the CT complex strengths and spectroscopic properties. The thermal behavior as revealed from DSC, of various enediynes was summarized in **Table 2**.

Table 2: DSC behavior of different enediynes containing D/D, D/A and A/A units

Compd. No	Aryl System	Onset Temp. (BC) °C	Compd. No	Aryl System	Onset Temp. (BC) °C
13	2-Naphthoxy (D) 2-Naphthoxy (D)	168	20	4-Methoxy-1-naphthoxy (D) 4-Nitro-3-trifluoromethyl phenoxy (A)	121
14	4-Nitrophenoxy (A) 4-Nitrophenoxy (A)	210	21	4-Methoxy-1-naphthoxy (D) 4-Nitrophenoxy (A)	152
15	2-Naphthoxy (D) 4-Nitrophenoxy (A)	161	22	Anthracene-9-methoxy (D) Anthracene-9-methoxy (D)	159
16	4-Methoxy-1-naphthoxy (D)	135	23	2,4-dinitrophenoxy (A) 2,4-dinitrophenoxy (A)	180

	4-Methoxy-1-naphthoxy (D)				
17	4-Cyano-2-nitrophenoxy (A) 4-Cyano-2-nitrophenoxy (A)	245	24	Anthracene-9-methoxy (D) 2,4-dinitrophenoxy (A)	125
18	4-Nitro-3-trifluoromethyl phenoxy (A) 4-Nitro-3-trifluoromethyl phenoxy (A)	205	25	Anthracene-9-methoxy (D) 4-Nitro-3-trifluoromethyl phenoxy (A)	119
19	4-Methoxy-1-naphthoxy (D) 4-Cyano-2-nitrophenoxy (A)	126	26	Anthracene-9-methoxy (D) Anthracene-9-methoxy-Picrate (A)	138

4. ENEDIYNE AS A SCAFFOLD FOR β -TURN PEPTIDOMIMETICS

As a part of our ongoing efforts to prepare scaffolds for β -turn peptidomimetics as well as metal ion specific peptides, we have designed and synthesized a pentapeptide **27** (Figure 5) where a novel enediynyl ω -amino acid is acting as fluorophoric reporter. The reason behind the design was two fold: a) to use the Z-enediynes moiety as a nucleator for β -turn peptidomimetic and b) to exploit and elaborate further, the intrinsic fluorophoric properties of this moiety simultaneously.

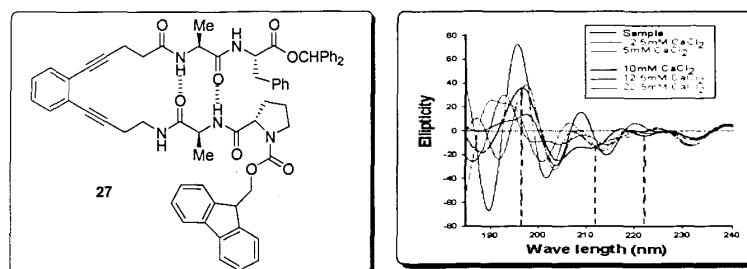
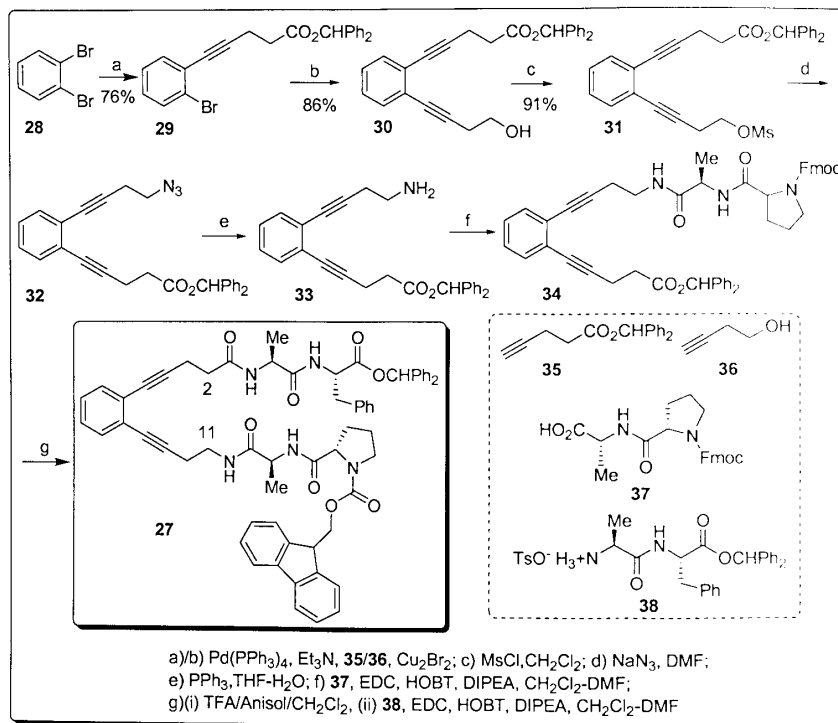


Figure 5: The Target Pentapeptide **27** (left) and its Overlaid deconvoluted CD spectra (333mM) in MeOH in absence and presence of various amounts of CaCl_2 (right).

To our knowledge, this is the first report of application of the intrinsic fluorophoric property of Z-enediynes in monitoring binding process of metal ions and colloidal gold nano particles.



Scheme 1: Synthesis of Novel enediynyl pentapeptide **27**

The key step in the synthesis of **27** is the preparation of the enediynyl amino acid in carboxy-protected form **33**. This was accomplished by sequential Pd (0)-mediated Sonogashira coupling (**Scheme 1**) in which Et₃N was used as solvent and as base because the use of traditional n-BuNH₂ proceeded with the formation of internal amide bond formation by cleaving the acid protecting group, the benzhydryl. The two arms were then extended using the partially protected dipeptides Ala-Pro (**37**) and Ala-Phe (**38**) via standard EDC mediated coupling protocol to furnish the target N, C-diprotected pentapeptide **27** [Fmoc-Pro-Ala-Eda-Ala-Phe-COOCHPh₂, where Eda = enediyne amino acid] as a pale brown solid. The ¹H NMR spectrum was recorded in CDCl₃ and all the proton signals could be assigned using extensive 2D NMR

experiments. The structure of the pentapeptide **27** was confirmed by NMR and Mass spectrometry.

The secondary structure of peptide **27** was estimated by recording its CD spectrum in methanol which showed a strong maximum at ~198 nm followed by several broad minima at ~205, 212 and 222 nm indicating that the peptide predominantly adopts a β -turn like structure (**Figure 5**) at least in the solvent used for the study. The turn like structure is more or less maintained in presence of Ca^{2+} ions.

The existence of β -turn implies the possible presence of intramolecular H-bond between the peptide strands on the two arms of the enediyne framework. This was assessed by determining the variation of chemical shifts of the various NHs with temperature in d_6 -DMSO. Variable Temperature NMR showed that among the four amide NH's, one alanine NH and the NH belonging to the enediynyl amino acid exhibited $\Delta\delta/\Delta T$ values that are within the Kessler limit¹³ of -3 ppb/K indicating strong intramolecular H-bonding and supported the predominant turn like structure of the peptide. The appearance of a cross peak for the hydrogens attached to C-2 and C-11 in NOESY spectrum also provided further evidence for the turn like conformation of the two peptide arms. The H-bonded conformation was also supported by the semi empirical AM1 geometry optimization.

The photophysical properties of **27** and possible perturbation by different metal ions were studied. The peptide itself in TFE showed emission at λ_{max} 380 nm when excited at 320 nm with a large Stoke shift (60 nm), a characteristic emission of enediyne moiety. For better understanding the fluorescence phenomenon we have first observed the emission at low temperature. No phosphorescence could be detected in the solvent (TFE) at 77K indicating that the emission arises due to $S_1 \rightarrow S_0$ fluorescence. At 77K a blue shift of about 12 nm is observed in TFE.

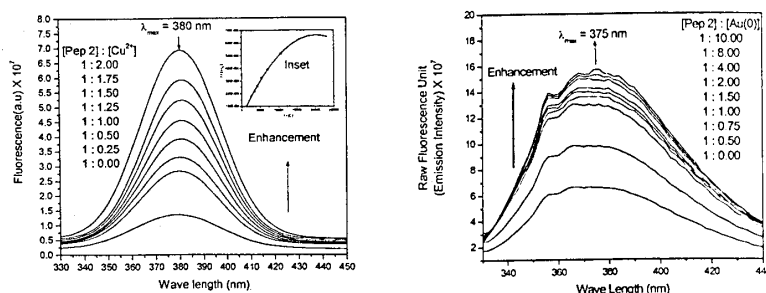


Figure 6: Fluorescence emission spectra of Cu (II) and Au(0) titration of peptide 27. Excitation wave length was 320 nm. Initial conc. of 27 was 1.87×10^{-5} M in TFE and of Au (0) was 10^{-3} M in THF

There were significant changes in fluorescence intensity upon addition of metal ions and gold nano particles. Transition metal ions all caused enhancement of fluorescence intensity with the extent of enhancement depending upon the nature of the metal ions added. The order of K (association constants) and Φ is $\text{Co(II)} \cong \text{Zn(II)} > \text{Cu(II)} > \text{Ni(II)}$. Fluorescence titration experiment (Figure 6) with Cu^{2+} ion showed that the peptide binds more than one Cu^{2+} ion as is evident from the nonlinear plot of $1/[I-I_0]$ vs. $1/[C]$ (inset). This result was also supported from MALDI ToF Mass spectrometry, the expected molecular ion peak, corresponding to the peptide and two Cu^{2+} ions, was observed. For the other metal ions, a linear plot revealed 1:1 complex formation.

The fluorescence behavior in the presence of alkali and alkaline earth metal ions is even more interesting. When the ratio of peptide to metal ion was kept at 1:1, fluorescence quenching was observed. At peptide-metal ion ratio of 1:2, enhancement of fluorescence of varying degree was observed. Interestingly, strongest enhancement was shown for K^+ ions while Na^+ and Ca^{2+} showed weak enhancement.

Observing the fluorescence perturbation by mono-valent and di-valent metal cations we were interested to know whether zero valent metal is able to cause any fluorescence perturbation or not. For this purpose we studied the changes in fluorescence intensity upon addition of Au(0)-nano particle in dry THF solvent. Interestingly we observed the enhancement of fluorescence intensity (Figure 6) as the concentration of nano particle was increased. To the best of our knowledge, up to now there have been only two reports about the gold-nanoparticle-enhanced emission from the fluoroprobe has been observed.

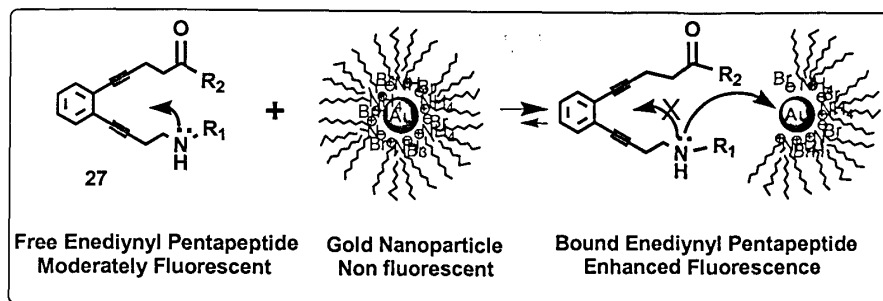
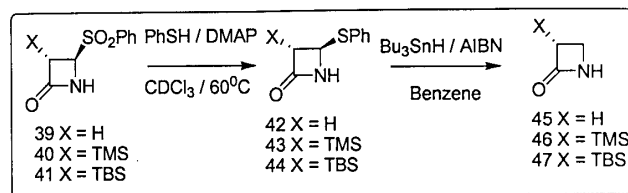


Figure 7: Probable mode of Fluorescence enhancement by gold nano particle

In conclusion, we have shown for the first time the use of an enediyne moiety as a probe for fluorescence studies. Thorson *et al.* have recently described the application of "molecular break lights" to develop the first continuous assay for cleavage of DNA by enediynes; however, they have used an external fluorophore for the assay. Our work adds a future prospect to study continuous DNA cleavage assay by monitoring the fluorescence intensity of active enediyne itself. The enediynyl peptide **27** is capable of binding strongly to transition metal ions and also to the colloidal gold nano particles with enhancement of fluorescence intensity. These findings have opened a new dimension of possible use of enediynyl peptides as chemosensors.

5. ROLE OF SILICON AT C-3 ON THE KINETICS OF DISPLACEMENT AT C-4 IN 2-AZETIDINONES

The conversion of proclavamate to clavamate by CS is a two-step process involving 4 electron oxidations. The first oxidation has been unambiguously proved to be the formation of C4-O bond to form the dihydroclavamate. Several studies have been carried out to know the nature of intermediate, a radical or cation, involved in such a conversion; however, a definitive answer is still to be found. A radical mechanism is however the preferred one, in analogy to similar enzyme mediated transformations. Various model studies concerning β -secondary kinetic isotope effect showed that the effect is suppressed in β -lactam system. Since silicon has a strong beta effect, we thought it would be worthwhile to study the effect of a silicon substituent at C-3 on reactions involving a cation or a radical at C-4 (**Scheme 2**). This study may throw some light on the involvement of antiaromaticity in these systems as well as the nature of oxygen insertion at C-4 in the actual enzymatic reaction pathway.



Scheme 2: Kinetics of nucleophilic and radical displacement

Both the reactions followed the pseudo first order kinetics. We observed that the β -effect is nonexistent in case of cation while for the radical some rate enhancement was observed. The magnitude of the β -stabilization was, however, much less than expected (calculated β -stabilization energy is ~ 3.2 KJ/mole as against 12.3 KJ/mol reported for 2-Trimethylsilyl-2-methyl propyl radical). Our result is also supported by theoretical calculation using Gaussian 98, ROMP2=FC/6-31G**//B3LYP/3-21G* level.

6. MOLECULAR SELF-RECOGNITION IN MONOCYCLIC β -LACTAMS: ROLE OF WEAK INTERACTIONS

The discovery of biologically active monocyclic β -lactams or monobactams, which are reported to be planar, has casted serious doubts regarding the strain theory. The intrinsic reactivity of a β -lactam may not be an index for its activity towards transpeptidase or β -lactamase enzymes; it is the weak non bonding interactions between the substrate and the enzyme which provide molecular recognition and binding energy to lower the activation barrier for interaction with target enzymes. Useful information may be obtained regarding the influence of weak interactions like H-bonds and hydrophobic interactions by studying the crystal structures of β -lactams. With this intention, we synthesized four monocyclic β -lactams, namely 4-phenyl sulphonyl 2-azetidinone **39** and its 3-methyl and 3, 3-dimethyl derivatives **48** and **49** respectively as well as the azetidinone **50** and studied their crystal packing to ascertain what type of forces are important in such self-recognition process.

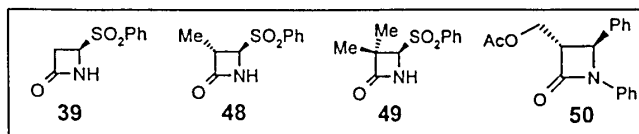


Figure 8: Our target β -lactams to study molecular recognition

Single crystal X-ray structures 39, a 1:2 conglomerate of 48 and 49a/49b and 50 were determined which revealed interesting variation in crystal packing dictated by H-bonding and hydrophobic interactions. This study reveals that the molecular recognition of the β -lactam derivatives may involve hydrophobic interactions and hydrogen bonding like N-H...O=C and N-H...O=S depending upon the orientation of the molecules in an assembly.